Title

Radiocarbon bomb-peak signal in tree-rings from the tropical Andes register low latitude atmospheric dynamics in the Southern Hemisphere

Authors

Ancapichún, Santiago
De Pol-Holz, Ricardo
Christie, Duncan A
et al.

Publication Date

2021-06-01

DOI

10.1016/j.scitotenv.2021.145126

Peer reviewed

Science of the Total Environment 774 (2021) 145126

Contents lists available at ScienceDirect

Science of the Total Environment

journal homepage: www.elsevier.com/locate/scitotenv

Radiocarbon bomb-peak signal in tree-rings from the tropical Andes register low latitude atmospheric dynamics in the Southern Hemisphere

Santiago Ancapichún [a], Ricardo De Pol-Holz [b,*], Duncan A. Christie [c,d], Guaciara M. Santos [e], Silvana Collado-Fabbri [f], René Garreaud [d,g], Fabrice Lambert [d,h], Andrea Orfanoz-Cheuquelaf [d,g], Maisa Rojas [d,g], John Southon [e], Jocelyn C. Turnbull [i,j], Pearce Paul Creasman [k]

[a] Postgraduate School in Oceanography, Faculty of Natural and Oceanographic Sciences, Universidad de Concepción, Concepción, Chile
[b] Centro de Investigación GAIA Antártica (CIGA) and Network for Extreme Environment Research (NEXER), Universidad de Magallanes, Punta Arenas, Chile
[c] Laboratorio de Dendrocronología y Cambio Global, Instituto de Conservación Biodiversidad y Territorio, Universidad Austral de Chile, Valdivia, Chile
[d] Center for Climate and Resilience Research (CR)2, Chile
[e] Department of Earth System Science, University of California, Irvine, USA
[f] Fundación Crono Austral, Concepción, Biobio, Chile
[g] Department of Geophysics, Universidad de Chile, Santiago, Chile
[h] Department of Physical Geography, Pontificia Universidad Católica de Chile, Santiago, Chile
[i] GNS Science, Rafter Radiocarbon Laboratory, Lower Hutt, New Zealand
[j] CIRES, University of Colorado at Boulder, USA
[k] American Center for Oriental Research (ACOR), Amman, Jordan

HIGHLIGHTS

- The world's highest elevation tree records the ^{14}C produced by nuclear detonations in northern latitudes during the 1960s
- During the initial ^{14}C spike, there were reversals on the north-south atmospheric $\Delta^{14}C$ gradient in the southern hemisphere
- Air parcel trajectories show that altitude and carbon provenance influenced the atmospheric $\Delta^{14}C$ in Tropical South America

GRAPHICAL ABSTRACT

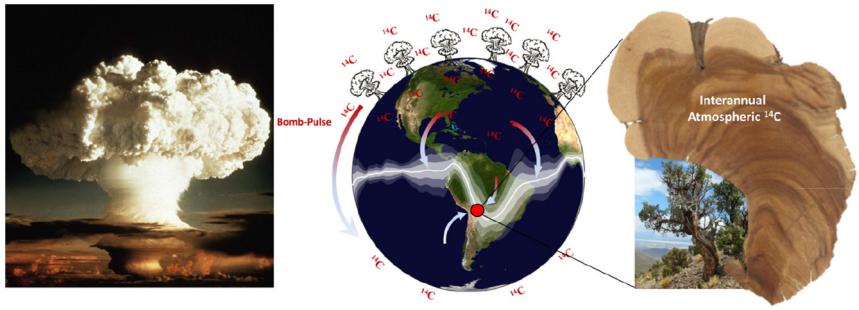

ARTICLE INFO

Article history:
Received 26 November 2020
Accepted 9 January 2021
Available online 6 February 2021

Editor: Martin Drews

Keywords:
Radiocarbon
Tree-rings
Southern hemisphere
Carbon reservoir effect
Atmospheric circulation

ABSTRACT

South American tropical climate is strongly related to the tropical low-pressure belt associated with the South American monsoon system. Despite its central societal role as a modulating agent of rainfall in tropical South America, its long-term dynamical variability is still poorly understood. Here we combine a new (and world's highest) tree-ring ^{14}C record from the Altiplano plateau in the central Andes with other ^{14}C records from the Southern Hemisphere during the second half of the 20th century in order to elucidate the latitudinal gradients associated with the dissemination of the bomb ^{14}C signal. Our tree-ring ^{14}C record faithfully captured the bomb signal of the 1960's with an excellent match to atmospheric ^{14}C measured in New Zealand but with significant differences with a recent record from Southeast Brazil located at almost equal latitude. These results imply that the spreading of the bomb signal throughout the Southern Hemisphere was a complex process that depended on atmospheric dynamics and surface topography generating reversals on the expected north-south gradient in certain years. We applied air-parcel modeling based on climate data to disentangle their different geographical provenances and their preformed (reservoir affected) radiocarbon content. We found that air parcel

* Corresponding author at: Centro de Investigación GAIA-Antártica, Domo Antártico, Universidad de Magallanes, Av. Bulnes, 01855 Punta Arenas, Chile.
E-mail address: ricardo.depol@umag.cl (R. De Pol-Holz).

https://doi.org/10.1016/j.scitotenv.2021.145126

trajectories arriving at the Altiplano during the bomb period were sourced i) from the boundary layer in contact with the Pacific Ocean (41%), ii) from the upper troposphere (air above the boundary layer, with no contact with oceanic or continental carbon reservoirs) (38%) and iii) from the Amazon basin (21%). Based on these results we estimated the $\Delta^{14}C$ endmember values for the different carbon reservoirs affecting our record which suggest that the Amazon basin biospheric ^{14}C isoflux could have been reversed from negative to positive as early as the beginning of the 1970's. This would imply a much faster carbon turnover rate in the Amazon than previously modelled.

1. Introduction

Tree-rings have proven to faithfully record the ^{14}C content of the adjacent atmosphere, a powerful tracer for the study of atmospheric circulation, exchanges between carbon reservoirs such as the oceans and the biosphere, ocean circulation, natural and man-made carbon emissions (Suess effect and nuclear power plants), and the global carbon cycle (Broecker et al., 1980; Hou et al., 2020; Hughen et al., 2004; Oeschger et al., 1975; Turnbull et al., 2006; Turnbull et al., 2009; Geller et al., 1997; Graven et al., 2012; Hesshaimer and Levin, 2000; Krakauer et al., 2006; Levin et al., 2010; Nydal and Lövseth, 1965; Nydal, 1968; Patra et al., 2011; Randerson et al., 2002; Hua et al., 2012). This is particularly so in the decade from the mid-1950s to the mid-1960s, when atmospheric radiocarbon levels almost doubled due to the large number of atmospheric thermonuclear bomb tests detonated in the northern hemisphere (NH) (Manning et al., 1990). The anthropogenically produced ^{14}C accumulated in the NH stratosphere and then gradually entered the troposphere via stratosphere-troposphere exchange processes at mid-to-high latitudes (Nydal and Lövseth, 1965). Once in the Equatorial troposphere, the air masses from the NH carrying the bomb-^{14}C signal were mixed with the low-^{14}C concentration air masses from the Southern Hemisphere (SH) (Lal and Rama, 1966; Nydal, 1968) through the latitudinal displacement of the Intertropical Convergence Zone (ITCZ). Thus, a large and persistent latitudinal gradient was generated around the globe during the so-called "bomb-period" (1950–1985; Hua et al., 2013).

Using tree-rings, Hua et al. (2012) found that atmospheric ^{14}C over Indonesia (5°S; Fig. 1), was markedly higher than over the southern latitudes during the austral summer (December, January, and February; DJF). The authors suggested that the influence of high ^{14}C-concentration northern air-masses enriched atmospheric ^{14}C above Indonesia (5°S; Fig. 1). The findings have meaningful paleoclimatic implications, since they establish the potential of atmospheric ^{14}C to trace changes on atmospheric patterns such as the shape and latitudinal variability of the ITCZ. Over large continental masses like Tropical South America (TSA), however, the narrow zonally extended ITCZ is not present and the atmospheric equivalent of a climatic equator is a ubiquitous tropical low-pressure belt (TLPB). During the austral summer, at the mature phase of the South American Monsoon (Fletcher, 1945; Tomas et al., 1999; Hastenrath and Polzin, 2004; Vuille et al., 2012), the TLPB reaches its southernmost latitudinal position above TSA –sometimes extending as far as 30° S, forming a 'U-shape' that encompasses the Amazon basin with a marked space-time variability (Fig. 1). Therefore, well suited tropical ^{14}C archives have the potential to record past atmospheric circulation changes associated with the TLPB. However, ^{14}C studies in TSA are scarce because most of the tree-ring studies have been developed at mid to high latitudes (Boninsegna et al., 2009; Oliveira et al., 2009, 2010). Presently, the most complete ^{14}C-record for TSA is located in Brazil (22° S, 46°W; Santos et al., 2015), which shows similar ^{14}C values for the bomb-period than those from higher latitudes of the SH despite being under the influence of the TLPB (Fig. 1). This evidences that latitudinal atmospheric ^{14}C differences not only depending on the latitudinal location of the record relative to the TLPB, but also the potential effect of different carbon reservoirs. We believe it is crucial to provide new and continuous atmospheric ^{14}C record for TSA, especially from the period when the bomb-^{14}C excess amplified the signal of atmospheric-flow patterns and carbon reservoir effects (Hua et al., 2012; Heimann and Maier-Reimer, 1996; Key et al., 2004; Naegler and Levin, 2009).

Polylepis tarapacana, is a long-lived (≥700 years) tree species with well-defined annual rings extensively utilized for dendroclimatic studies (Morales et al., 2020). *P. tarapacana* inhabits the Altiplano (15–23°S; 68°W), a high-altitude semiarid plateau at 4000 m above sea level (asl) in the tropical central Andes, and is considered the world's highest elevation tree. Besides these exceptional features, *P. tarapacana* is under the influence of particular atmospheric-flow

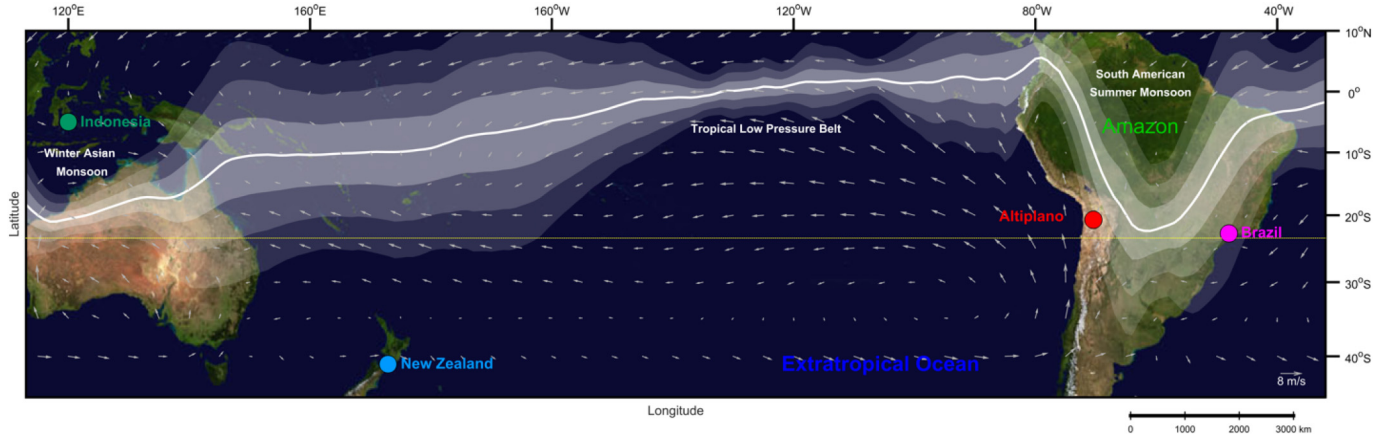

Fig. 1. Locations of $\Delta^{14}C$ records used in our study: Altiplano (*Polylepis tarapacana*; 20°S, red dot, this study); Indonesia (*Tectona grandis*; 5° S, green dot; Hua et al., 2012); Brazil (*Araucaria angustifolia*; 22° S; magenta dot; Santos et al., 2015); and New Zealand (atmospheric measurements from Wellington; 41°S, blue dot; Turnbull et al., 2017). The white line represents the average ($\pm$ 1 σ, $\pm$ 2 σ, and $\pm$ 3 σ) latitudinal positions of the Tropical Low-Pressure Belt (TLPB) drawn following the 1949–2019 averaged austral summer (DJF) minimum sea level pressure between 10° N and 35° S in the NCAR/NCEP reanalysis. White vectors show wind velocity and direction. The Tropic of Capricorn is shown with the yellow dotted line.

patterns. The Altiplano separates the dry Atacama Desert from the wet influences of the Atlantic, which support the world's largest rainforest in the Amazon basin (Fig. 1) (Garreaud et al., 2003). Locally, during DJF, the radiative heat from the Altiplano warms surface air masses, which ascend and enable the intrusion of moist air masses from the east, specifically from the Amazon basin, reducing the intrusion of dry air masses from the west and causing 70–90% of the Altiplano annual precipitation (Vuille et al., 2000; Vuille and Keimig, 2004; Garreaud et al., 2009). On a broader scale, Segura et al. (2020) identified a meridional circulation associated with the vertical flow of the western Amazon convection that also affects the moisture transport towards the Altiplano.

Considering the U-shape of the TLPB, with its western flank coincident with the central Andes, air parcels arriving at the Altiplano from the northeast originated to the north of the TLPB are relatively wet and should have carried the bomb-^{14}C excess derived from nuclear testing. By the contrary, air parcels arriving to the Altiplano from the west (especially from the southwest) originated outside the TLPB and should carry low-moisture and low-^{14}C concentration from the extratropical SH. We thus expect that an increase in the arrival of eastern air parcels from the TLPB influence-region caused an increase in the atmospheric ^{14}C recorded by *P. tarapacana* relative to another SH records. To test our hypothesis and to get a better understanding of atmospheric ^{14}C variability over TSA, we have measured ^{14}C in *P. taparacana* annual rings from the bomb-period (1950–1985), compared it with other relevant SH ^{14}C records, and modelled the tropical atmospheric circulation in order to elucidate the main carbon reservoirs that could be affecting the *P. tarapacana* signal.

2. Materials and methods

2.1. Altiplano tree-ring samples and radiocarbon analyses

P. tarapacana (Queñoa) is a small tree from the *Rosaceae* family with well-defined annual rings that grows at high altitudes (4000–5000 m asl) in the Central Andes region of Peru, Chile, Bolivia and Argentina. We sampled ^{14}C in the annual rings of a *P. tarapacana* during the 1950–1985 period from the Irruputuncu tree-ring site located at 4324 m asl within the Altiplano region (20°S, 68°W). The Irruputuncu *P. tarapacana* tree-ring chronology was previously developed by cross-dating 111 tree-ring series within the site comprising 30,620 annual rings (Morales et al., 2020), and corroborated its annual resolution against 16 different *P. tarapacana* tree-ring sites which encompass 929 tree-ring series and 209,820 annual rings of the species across the Altiplano (Christie et al., 2009; Solíz et al., 2009; Morales et al., 2012; Morales et al., 2015; Lima et al., 2016). Also, independent historical records from severe droughts and pluvials have been used to corroborate the annual nature of the *P. tarapacana* tree-ring network (Morales et al., 2020). Sample preparation was done by cutting dated tree-rings under a binocular microscope into annual rings using sterile ceramic knives over an acrylic table at the tree-ring lab of the Universidad Austral de Chile. Each annual wood segment was polished with diamond tools to remove the surface that was in contact with extraction and sanding tools. For studying post-bomb ^{14}C in tree-rings at annual resolution, it is extremely important to isolate the carbon assimilated in the corresponding growth year, as non-cellulosic compounds can be synthesized the year after the ring formation or can be translocated between several rings (Anchukaitis et al., 2008; Santos et al., 2020). Therefore, we extracted the holocellulose of each *Polylepis* ring for ^{14}C measurements as it has been shown to be a useful way to remove any mobile carbon from other years (Capano et al., 2017; Santos et al., 2020). Briefly, tree-ring samples were chemically cleaned by a series of acid-base washes followed by the removal of lignin and other mobile carbon fractions through chlorine baths (Southon and Magana, 2010). The holocellulose was then combusted, and CO_2 was cryogenically separated and reduced to graphite by H_2 using FeO as a catalyst (Santos and Ormsby, 2013). The ^{14}C content of the graphite sample was measured at the AMS facility of the University of California at Irvine (Santos et al., 2004, 2007). Radiocarbon results are reported as Δ^{14}C values that are corrected for known age to 1950 according to convention (Stuiver and Polach, 1977). *P. tarapacana* growth is strongly related to temperature and precipitation occurring between December and February (DJF), therefore we assigned the calendar age of each ring as the SH dendro age plus one; e.g. the atmospheric ^{14}C stored in growing season of 1949–1950 was assigned to January 1st 1950. We use IAEA-C3 (cellulose) as well as holocellulose extracted from wood shaved from tree-rings of *Sequoia sempervirens* centered in year 1850 as secondary standards. Our full *P. tarapacana* Δ^{14}C record spans from 1950 to 2014, however, for the purpose of this article, we present here the data from 1950 to 1985. We measured replicates of >10% of the samples and calculated error weighed averages for those years with more than one data point (Supplementary information). The pooled standard deviation based on all replicates produced for the 1950–2014 record is 5‰, whereas the higher variability associated with the 1950–1972 period increases our pooled standard deviation to 6.1‰.

2.2. Geographical provenance of air parcels

We used HYSPLIT to assess the potential geographical provenance of the air parcels that transported the $^{14}CO_2$ that was subsequently fixed in the *P. tarapacana* (and *A. angustifolia*) tree-rings (Draxler and Hess, 1998; Draxler and Stunder, 1988; Stein et al., 2015). The HYSPLIT model v.4 is a complete system designed to calculate simple air-parcel trajectories, complex transport, dispersion, chemical transformation, and depositional simulations. The NCEP/NCAR reanalysis was used as the input data of the HYSPLIT model (Kalnay et al., 1996). This is the only comprehensive climatological dataset covering the beginning of the bomb-testing period, and it is based on in situ observations and satellite data which have been proven to be reliable for the representation of atmospheric variables (Kalnay et al., 1996). On the other hand, the backward trajectories calculated using HYSPLIT are generated as a set of longitudinal, latitudinal, and altitudinal points based on an arbitrary number of hours into the past for a specific hour of the day (Draxler and Taylor, 1982). Previous studies have shown that 120 h (5 days) is a suitable time-window to overcome potential biases since shorter time-windows tend to show limited trajectories that are too close to the study site, and longer time-windows may be associated with major propagation errors (Scarchilli et al., 2011; Schlosser et al., 2008; Sinclair et al., 2013). A 5-day time window allows for ~35% of the original CO_2 to be exchanged with the local reservoir with the concomitant effect on the Δ^{14}C of the air parcel (supplementary information). In this way, we calculated 24 backward trajectories (one for each hour of the day) for each day of the growing season (December to February) between the years 1950 and 1985 (77,760 computed trajectories by each TSA record). Each backward trajectory describes the spatial displacement of air parcels during the 5-day time-window (see supplementary information for details).

In order to determine the latitudinal limits of the TLPB-influence and its space-time variability, we used the above sea-level pressure data from the National Center for Environmental Prediction/National Center for Atmospheric Research (NCEP/NCAR) Reanalysis dataset (Kalnay et al., 1996) (see supplementary information). Based on the air parcel position at hour −120, we detected three main geographical provenances that could have a potential isotopic fingerprint, i.e. Amazon basin, the lower troposphere over the extratropical Pacific Ocean and upper troposphere. The criteria for assigning air parcels to each of these geographical provenances is the following: i) air parcels that at hour −120 are located at a more northerly latitude than the average-location of the TLPB – 2σ were assigned to the Amazon basin; ii) air parcels that at hour −120 are located to the south of the average-shape of the TLPB – 2 σ were assigned to the extratropical ocean and iii) the air parcels that at hour −120 are located at higher altitudes than the

different atmospheric boundary layers (see Supplementary Information for details) were assigned to the upper troposphere. The contribution of air parcels from a geographical provenance is gauged by the percentage given by the number of air parcels positioned above a particular geographical provenance at hour −120 relative to the total number of air parcels in all of the backward trajectories.

2.3. $\Delta^{14}C$ endmembers

We use the term '$\Delta^{14}C$ endmember' to represent the preformed ^{14}C content of air parcels that characterizes a particular geographical provenance. In theory, air parcels from the TLPB influence-region must have a higher ^{14}C concentration than air parcels at latitudes further south than the TLPB influence-region. On the other hand, when a carbon reservoir exchanges CO_2 with its adjacent air parcel, this air parcel will acquire the $\Delta^{14}C$ fingerprint of the corresponding carbon reservoir. This influence of carbon reservoirs on air-parcels is called 'isoflux' (Turnbull et al., 2016). The isoflux is the product of the one-way gross CO_2 flux and the isotopic difference between the source (or sink) and the atmosphere. For example, if a given carbon reservoir has a significantly higher $\Delta^{14}C$ than the adjacent atmosphere, there will be a positive isoflux causing an increase in the $\Delta^{14}C$ of the adjacent air parcel; and vice versa. During the bomb-testing period, the produced atmospheric ^{14}C excess exacerbated the isofluxes of each carbon reservoir due to the amplified isotopic difference between the carbon sources and sinks.

To assess the endmember $\Delta^{14}C$ of each geographical provenance affecting the Altiplano, we first obtained the interannual percentage contribution of air parcels from each geographical provenance using HYSPLIT as discussed in the previous section. Then, we chose selected ^{14}C records that are expected to directly or indirectly express the endmembers of the geographical provenances. For this, we assume that the raw $\Delta^{14}C$ of the records are a combination of different fractions of air masses with their corresponding endmember $\Delta^{14}C$ and that each carbon reservoir exchange with the adjacent air masses is constrained to the altitude of the boundary layer (Graven et al., 2012; Levin et al., 2010; Randerson et al., 2002). The generic equation that is used (see Hua and Barbetti, 2007) on the different records to assess the endmember values is:

$$C = n_1E_1 + n_2E_2 + \ldots + n_iE_i \quad (1)$$

where C is the measured $\Delta^{14}C$ level for a specific site, E_i are the endmember $\Delta^{14}C$ levels for specific geographical provenances; and n_i are the associated fractions of air masses contribution of a geographical provenance; hence:

$$n_1 + n_2 + \ldots + n_i = 1$$

As discussed later on, the HYSPLIT model results showed that for the Altiplano, the main geographical provenances are (i) the SH Pacific extratropical ocean, (ii) the Amazon basin and (iii) the upper troposphere. One of these, the Pacific extratropical ocean, can be assessed by using direct atmospheric $\Delta^{14}C$ measurements from Wellington (DJF), New Zealand (41° S, 174° E) (Rafter and Fergusson, 1959; Turnbull et al., 2017). The Amazon basin endmember is then calculated by using the *Araucaria angustifolia* record from the Atlantic forest biome in Southeast Brazil (22° S, 46° W) (Santos et al., 2015), which is located at a similar latitude than *P. tarapacana*, but whose main air parcel geographical provenances are the SH Atlantic extratropical ocean and Amazon basin. Once the Amazon basin endmember is calculated we derive the upper troposphere using our *P. tarapacana* ^{14}C record. Considering that the southwest region of both Atlantic and Pacific Oceans share latitudinal location, climatic settings, and reservoir effect, we justify our selection assuming no significant differences in atmospheric $\Delta^{14}C$ (Hua et al., 2013).

3. Results and discussion

3.1. Atmospheric $\Delta^{14}C$ variability over the Altiplano and the SH

The new *P. tarapacana* ^{14}C record is shown in Fig. 2. As expected, the annual chronology faithfully captured the bomb signal both in terms of timing and magnitude. The period 1950–1960 is characterized by rapid swings in the Altiplano $\Delta^{14}C$, reflecting the complicated Andean mixing of the initial bomb signal during this decade (see Section 3.2). As shown by Turnbull et al. (2017), the bomb signal transported from the NH to the SH was lagged by about 1.4 years (one year according to our centering on 1st January; see supplementary information). The bomb-peak in the Altiplano is centered on the year 1966, occurring after large $\Delta^{14}C$-changes of more than 200‰ yr^{-1} during the period 1963–1966. This reflects the bomb-^{14}C excess produced by thermonuclear detonations in the NH, which resulted in local stratosphere $\Delta^{14}C$ values as high as 5000–20,000‰ (Hesshaimer and Levin, 2000). Then, during the boreal spring and summer, this ^{14}C excess gradually entered the troposphere of the NH, causing a large peak of atmospheric ^{14}C observed at 47° N, Austria, in the year 1964 (Fig. 2). This ^{14}C excess was subsequently transported south (Nydal, 1968), affecting first the equatorial region and then the Southern Hemisphere, reaching its maximum level there in 1965 (Indonesian record; Fig. 2). As a result of this, a large and persistent north-south $\Delta^{14}C$ positive gradient was present in the global troposphere between 1950 and 1972, which we call the 'maximum gradient period' (MGP; Hua et al., 2013). In order to assess the full geographical variability of the bomb signal in the SH, we constructed indices based on the ^{14}C differences between TSA tree-ring atmospheric $\Delta^{14}C$ records (Altiplano and Brazil) and two other records from locations representing different SH endmembers. These were *Tectona grandis* from Muna Island, southeast of Sulawesi, Indonesia (5° S, 122° E), located perennially north of the austral summer TLPB and strongly affected by the ^{14}C-enriched air masses of the NH and by the tropical ocean isoflux (Hua et al., 2012), and with air ^{14}C from Wellington, New Zealand, located perennially south of the TLPB and influenced by the negative extratropical ocean isoflux (Turnbull et al., 2017).

Fig. 3 shows 5 indices constructed by subtracting the lower minus higher latitude $\Delta^{14}C$ records, as well as the magnitude of bomb energy released to the atmosphere through atmospheric nuclear bomb tests. Negative values in our indices are indicative of reversals in the expected north-south positive gradient, and as such, they imply the influence of carbon reservoirs or air parcel pathways. Indeed, TLPB index I (Indonesia – Altiplano, Fig. 3a) shows some negative values during the beginning of the bomb peak (years 1950, 1951, 1956, and 1958), whereas the TLPB index II (Indonesia – Brazil, Fig. 3b) is almost always positive during the MGP. However, the TLPB index II (Indonesia – Brazil) shows negative values between 1973 and 1978 (see Section 3.2). The Altiplano tree-ring record has $\Delta^{14}C$ values that were up to 25‰ higher than Indonesia, which points to an enriched source of ^{14}C arriving at high altitude in western TSA early in the bomb-period. The tropospheric altitude at which physical and chemical mixing occurs between the atmosphere and the Earth's surface varies between oceanic and continental regions; the marine and continental atmospheric boundary layers are located approximately 1 km and 1.5 km above the surface, respectively (Garratt, 1994; Zeng et al., 2004; Messager et al., 2012). Exchanges between carbon reservoirs and the lower troposphere are constrained to these boundary layers, and air parcels from the upper troposphere (higher altitudes than the upper limits of the boundary layers) have a different isotopic signal as they do not directly exchange CO_2 with the biosphere or the oceans, rather they are more influenced by long-range transport and also by natural cosmogenic ^{14}C production in the upper atmosphere. Therefore, considering the above and that several studies have described that high-altitude measurements have different $\Delta^{14}C$ levels than low-altitude measurements (Levin and Kromer, 2004; Turnbull et al., 2009; Graven et al., 2012), reversals in the expected north-south positive gradient

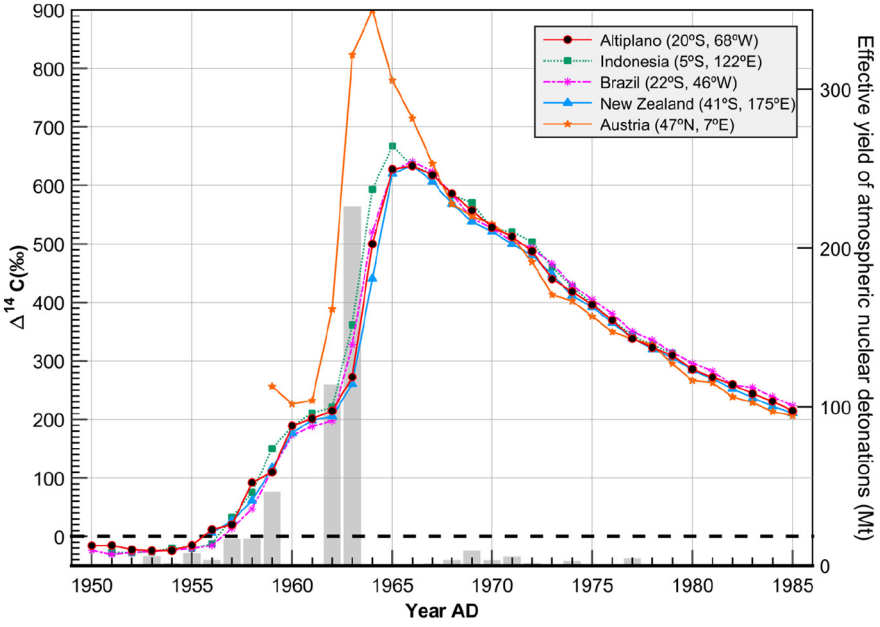

Fig. 2. *Polylepis tarapacana* annual ^{14}C during the bomb-testing period (red line with black circles) is shown. For comparison, we include the December, January, and February average of the monthly seasonally detrended atmospheric $\Delta^{14}C$ from New Zealand (Turnbull et al., 2017; light blue line with triangles), *Araucaria angustifolia* $\Delta^{14}C$ record from Brazil (Santos et al., 2015; magenta broken line with asterisks) *Tectona grandis* $\Delta^{14}C$ record from Indonesia (Hua et al., 2012; green dotted line with squares), and Austria atmospheric $\Delta^{14}C$ summer measurements (Levin and Kromer, 2004; orange solid line with stars) representative of the midlatitude northern hemisphere. The grey bars show the effective yield in megatons of thermonuclear detonations during this period which is directly related to the quantity of ^{14}C atoms generated (Enting, 1982).

found in the TLPB index I are likely explained by the influence of ^{14}C-enriched air parcels from the upper troposphere (see Section 3.2). Both indices show a prominent positive peak in 1964, indicating the high ^{14}C signal from the NH arriving in Indonesia with a lag of about 1 year from the maximum ^{14}C production from weapon testing.

The extratropical index I (Altiplano – New Zealand) (Fig. 3c) shows slightly positive or near-zero values during the MGP, as expected from the north-south positive global gradient (Hua et al., 2013), except for 1964 where the Altiplano record shows higher $\Delta^{14}C$ levels than New Zealand (60‰). However, Extratropical index II (Brazil – New Zealand) (Fig. 3d), shows slightly negative values during 1956–1962 and positive ones thereafter. This reversal in the expected pattern might be explained by the biospheric reservoir effect of the Amazon rainforest affecting the *A. angustifolia* site and/or a southern air parcel provenance. Naegler and Levin (2009) demonstrated that the radiocarbon isoflux from the biosphere to the troposphere was amplified from $-235 \pm 55‰\ yr^{-1}$ up to $-30{,}000 \pm 6000‰\ yr^{-1}$ near the start of the bomb-period. The ocean-troposphere isoflux was also highly amplified from $-5500 \pm 1400‰\ yr^{-1}$ during the pre-bomb-testing period to $-54{,}000 \pm 13{,}000‰\ yr^{-1}$ near the start of the bomb-period (Heimann and Maier-Reimer, 1996; Key et al., 2004). However, while the Southern Ocean had a dominant role on the ocean-troposphere isoflux, the sub-tropical ocean had a small negative isoflux. This occurred because of the natural radioactive decay of ^{14}C in old water masses that have been transported by the thermohaline circulation and have upwelled in the Southern Ocean, and because of the relatively shallow mixed layers and limited vertical entrainment of pre-bomb water masses in the mid-ocean gyres (Braziunas et al., 1995; Randerson et al., 2002). In fact, Randerson et al. (2002) modelled a zonal difference of the contribution of $\Delta^{14}C$ fluxes through the Amazon Rainforest and the Atlantic Ocean from the bomb-period, and theorized high tropospheric $\Delta^{14}C$ values over the tropical and extratropical Atlantic Ocean and low values over the Amazon Basin for the early bomb-period. This suggests that the Amazon biosphere-troposphere carbon exchange has played a dominant role in modulating the $\Delta^{14}C$ signal over Brazil. Therefore, reversals in the expected north-south positive gradient in extratropical Index II during the MGP can be explained by the more strongly negative isoflux generated by the carbon flux from the biosphere to the troposphere.

The TSA index (Altiplano – Brazil) (Fig. 3e), shows remarkably high variability throughout the MGP despite being almost a zonal gradient due to the similar latitude of both records. During the first part of the MGP, the index is characterized by positive values, but then a sharp decrease to very negative ones (up to −45‰) occurs right before the bomb peak, coinciding with the 1-year lagged bomb test maximum. These are clear indications of different air masses arriving in TSA at similar latitudes but different altitudes or different carbon-reservoirs affecting these air masses.

3.2. Air parcel ^{14}C affecting TSA tree-ring records

Based on the Altiplano and Brazilian tree-rings ^{14}C record locations, HYSPLIT geographical provenance results show that the bulk of air parcels arriving in TSA during the studied period came from the extratropical ocean and the TLPB influenced region of the Amazon basin (Fig. 4). Additionally, the Altiplano receives an important contribution of air parcels coming from the upper troposphere of the tropical Pacific (ca. > 3 km, figure 4ce). Quantitatively, 41% derive from the extratropical ocean, 38% from the upper troposphere, and 21% from the Amazon Basin. For the *A. angustifolia* record of Santos et al. (2015) in Southeast Brazil, our analysis shows that 53% of the air parcels arrive from the extratropical ocean, 38% from the Amazon Basin, and only 9% from the upper troposphere. These results highlight the fact that the Altiplano has an additional source of air parcels that could explain the observed ^{14}C differences with *A. angustifolia*. While the extratropical ocean is a dominant source for both records, the Amazon biosphere-troposphere carbon exchange has also played an important role in modulating the $\Delta^{14}C$ signal over TSA. Irrespective of the altitude, our findings show clear summer east-west flows that determine the provenance of air parcels for the Altiplano (Fig. 4a). This is in general agreement with previous studies of the atmospheric circulation in the area (Apaéstegui et al., 2018; Garreaud, 1999; Lenters and Cook, 1997; Perry et al., 2014; Vuille and Keimig, 2004; Vuille et al., 2000). The interannual variability of air parcel geographical provenance (Fig. 4g) shows that

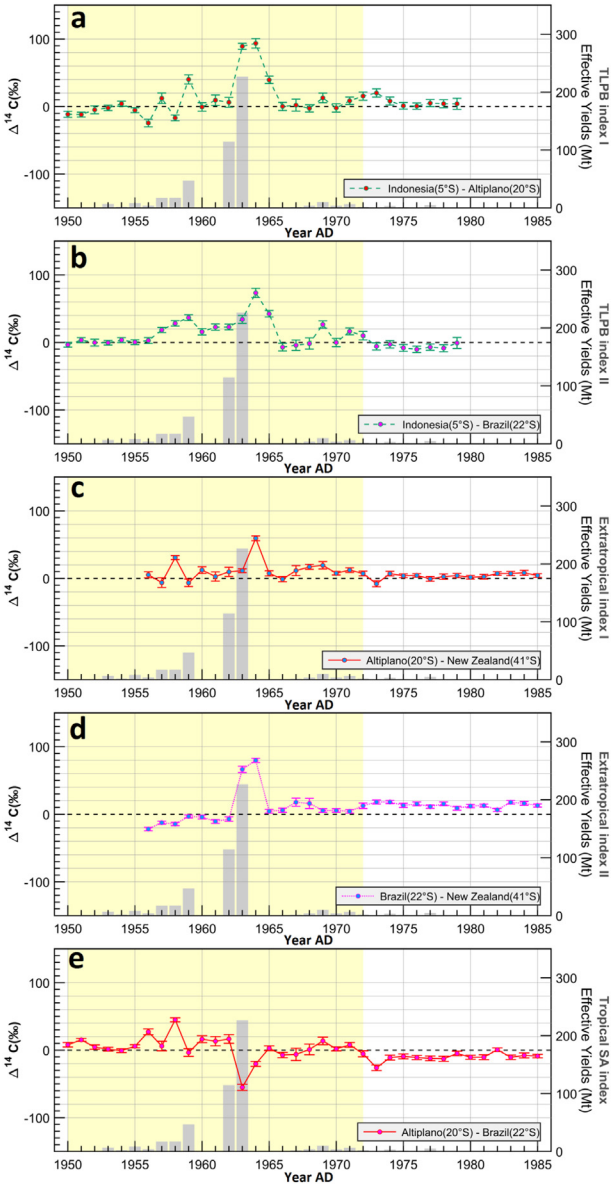

Fig. 3. Indexes based on latitudinal $\Delta^{14}C$ differences (north – south): (a) TLPB index I = Indonesia - Altiplano; (b) TLPB index II = Indonesia - Brazil; (c) Extratropical index I = Altiplano - New Zealand; (d) Extratropical index II = Brazil - New Zealand and (e) TSA index Altiplano - Brazil. Colored area is the Maximum Gradient Period (MGP, Hua et al., 2013) and the dashed black line indicates $\Delta^{14}C = 0$. The magnitude of nuclear explosions during the bomb-testing period is also shown (grey bars, based on Enting, 1982).

during the bomb-testing period, an increase in the upper-tropospheric contribution towards the Altiplano is associated with a decrease in contribution mainly from the extratropical Pacific Ocean and secondarily from the Amazon Basin. This pattern is corroborated by correlation analysis of interannual air-parcel geographical provenance series that show a significant negative relationship between the upper-tropospheric contribution towards the Altiplano with the contribution from both the extratropical Pacific Ocean ($R = -0.85$; $p < 0.05$) and the Amazon basin ($R = -0.58$; $p < 0.05$). These results could be related to the vertical flow pattern described by Segura et al. (2020), where an increase of the upward flow in the western Amazon and the Altiplano generates an increase in moisture transport from the Amazon basin. By extension, our analysis also shows that a decrease in the upper troposphere contribution towards the Altiplano implies an increase of upward flow not only from the Amazon (Neukon et al., 2015; Vera et al., 2019), but also an intrusion of air parcels from the Pacific Ocean lower-troposphere. This is a novel mechanism that will be studied in more depth in future research, given the importance to understanding rainfall events in the Altiplano.

To test our hypothesis that an increase in air parcels from the TLPB influence-region during the bomb period should cause an increase in ^{14}C in tree-rings of *P. tarapacana* and *A. angustifolia* relative to other SH records, we compared both TLPB and Extratropical indices of Fig. 3 with the percentage of air parcels arriving from the Amazon basin at both locations (Fig. 5a,b). If correct, our hypothesis predicts a decrease in the ^{14}C difference between Indonesia and TSA records (TLPB indices) when the % of air parcels from the Amazon basin increases. In other words, there should be a negative correlation between the amount of air arriving from the Amazon basin and the TLPB indices 1 and 2. Conversely, there should be a positive correlation between the amount of air arriving from the Amazon basin and the extratropical indices, i.e. the $\Delta^{14}C$ difference between TSA records and New Zealand. However, following a first approach using Pearson's correlation coupled with Monte-Carlo analyses done separately for the MGP and post-MGP periods, there are no significant relationships between the air parcels that arrive at the TSA-records from the Amazon basin and the $\Delta^{14}C$-indices (see Supplementary information). Despite this apparent lack of mechanistic causality, we further calculated the $\Delta^{14}C$ endmember values affecting the TSA tree-ring records in order to better understand the atmospheric $\Delta^{14}C$ variability over TSA.

Using the "Wellington smoothed" $\Delta^{14}C$ record (Turnbull et al., 2017) as representative of the extratropical ocean (both Pacific and Atlantic) endmember, we used the *A. angustifolia* ^{14}C data to solve for the Amazon basin endmember, ignoring the negligible contribution of the upper troposphere (~2 km) air parcels to that site. Subsequently, we use the calculated Amazon basin endmember together with the Wellington record and the Altiplano ^{14}C to solve for the upper troposphere endmember. The interannual evolution of these endmembers is shown in Fig. 5c. During the initial bomb rise (1956–1962), our estimated Amazon $\Delta^{14}C$ shows the most depleted endmember values affecting both TSA tree-ring records while the upper troposphere contributes with highly ^{14}C-enriched air parcels to the Altiplano. From 1950 to 1962 the Amazon air parcel contribution to both Brazil and the Altiplano is moderate, with both locations showing the extratropical ocean as an important source of air (Fig. 4 g,h). The low Amazon endmember values ($\Delta^{14}C < 0‰$) during the initial bomb-period are consistent with observational and model-based data that shows the effect of the biospheric negative ^{14}C isoflux on tropospheric air over the Amazon basin (Randerson et al., 2002) that could have lowered the original NH bomb signal. At the same time, the enriched northern sources affecting the upper troposphere during those years are probably related to bomb derived radiocarbon transported from the NH by the upward limb of the Hadley cell at the Equator and then to higher latitudes, without carbon-exchange with the SH ocean, to subsequently move downwards at the subtropics (20–30°S) (Rind et al., 2001; Held and Hou, 1980; Quan et al., 2004). The interplay of these two extremes, and the transient changes in air parcel geographical provenance contribution from ocean-dominated to upper troposphere-dominated, probably explains the rather variable $\Delta^{14}C$ over the Altiplano and the unexpected negative values of the TLPB index I for the period before 1960. Between 1963 and 1964, air parcels arriving at the Altiplano from the Amazon Basin had higher ^{14}C concentrations than the air parcels from the upper troposphere. As previously explained, these values are likely related to nuclear weapons testing and changes in the Amazon isoflux. The air parcels influencing the Brazilian tree-ring record were derived from lower altitudes and more northern latitudes than those arriving at the Altiplano. As such, the air parcels reflected in the Brazilian tree-ring record were more directly influenced by the bomb ^{14}C excess. Meanwhile the large negative Amazon isoflux observed during the early bomb-period was weakened, due to the gradual assimilation of bomb-^{14}C excess by the Amazon rainforest. Then, between 1965 and 1972 the Amazon and upper troposphere endmembers do not show large

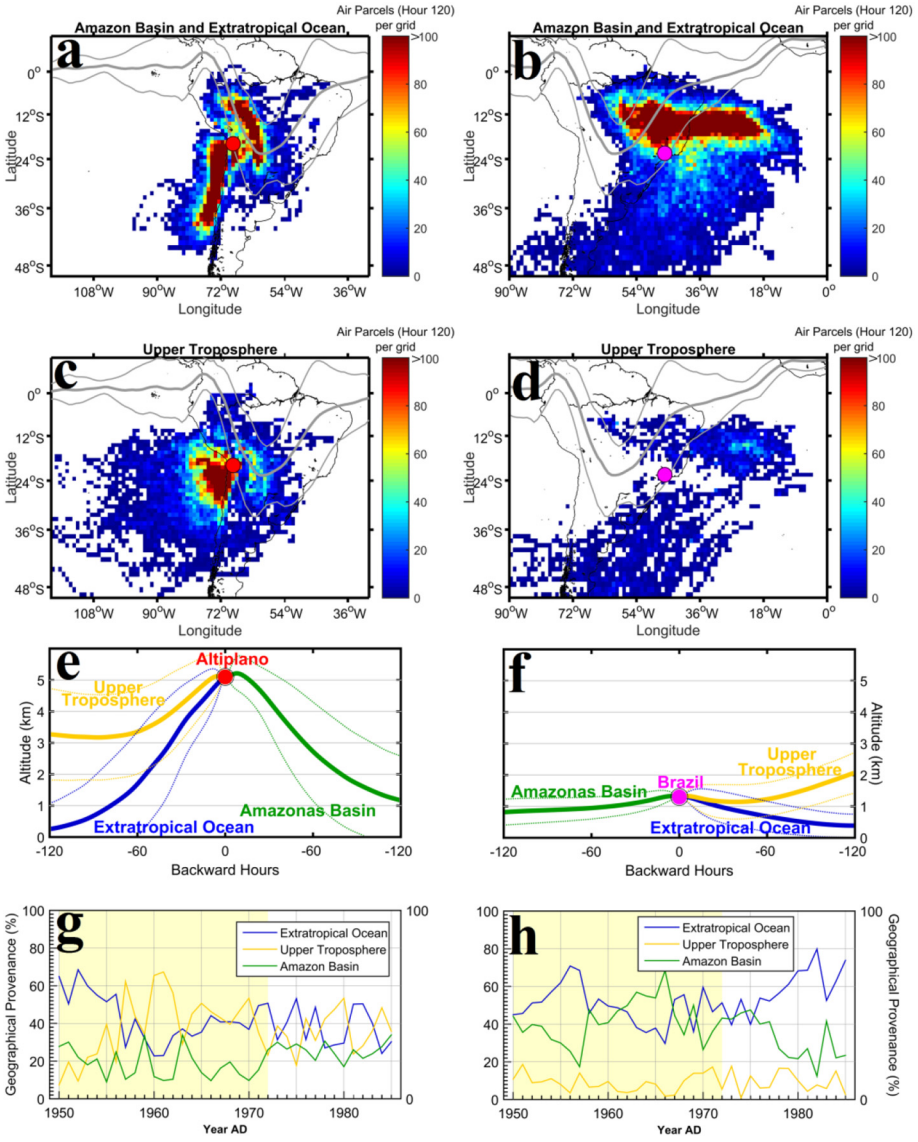

Fig. 4. HYSPLIT backward trajectory analysis results for TSA. (a) Air parcel density arriving to the Altiplano from within the atmospheric boundary layers (see Supplementary information). The colorbar scale indicates the total number of air parcels located on each pixel grid (1° × 1°) at hour −120 during the entire study period (DJF, 1950 to 1985). The solid grey lines show the mean temporal shape of the Tropical Low-Pressure Belt ±2σ of its spatial variability; (b) Same as (a) but for Southeast Brazil; (c) Same as (a); but for air parcels originating above the atmospheric boundary layers (see Supplementary information) (d) Same than (c) but for Southeast Brazil; (e) Mean altitude of the air-parcel trajectories that reached the Altiplano during the studied period (solid colour lines) and its standard deviation (dotted colour lines); (f) same that (e) but for Southeast Brazil; (g) air parcel contribution (%) of each geographical provenance arriving in the Altiplano during the studied period (h) same as (g) but for Southeast Brazil. The shaded yellow area highlights the maximum gradient period of 1950–1972.

differences. However, from 1973 onwards, the Amazon endmember turns into the highest source of enriched ^{14}C, notably after the MGP. Carbon cycle modeling studies have suggested that the reversal (from negative to positive) of the Amazon biospheric isoflux occurred during the mid-80s as enriched bomb ^{14}C from previous decades was respired (Levin et al., 2010; Randerson et al., 2002). Our calculated Amazon endmember, however suggests that this reversal could have happened at least 10 years earlier. Although preliminary, new ^{14}C data from *Cedrela odorata* from the northeastern sector of the Amazon basin also point to an earlier isoflux reversal (Santos, unpublished results). Reasons for this discrepancy might be the coarse resolution of the modeling framework that could underestimate the carbon reservoir effect of the Amazon biosphere (Randerson et al., 2002) and/or the soil carbon turnover times that are poorly constrained in the model considering the large Amazon respiration fluxes (Fan et al., 1990). Therefore, our results strongly suggest that when comparing the bomb signal in tree-ring records from different latitudes, the disruption on the expected north-south positive $\Delta^{14}C$ gradient global pattern could be associated to the altitude of a record, atmospheric circulation, and the carbon reservoirs upwind to the record.

4. Conclusions

The new *P. tarapacana* ^{14}C record faithfully captured the bomb signal both in terms of timing and magnitude. Atmospheric $\Delta^{14}C$ offsets between TSA and SH records provide evidence that the expected north-south positive $\Delta^{14}C$ gradient global pattern did not always occur. Despite being broadly applicable, global zoning according to regional $\Delta^{14}C$ concentrations and superficial atmospheric circulation is an oversimplification that needs to be reevaluated.

Our air parcel analyses demonstrated that TSA ^{14}C records are influenced by air parcels from three different geographical provenances. In agreement with previous studies, our $\Delta^{14}C$ estimations from these three geographical provenances suggest an important signal associated

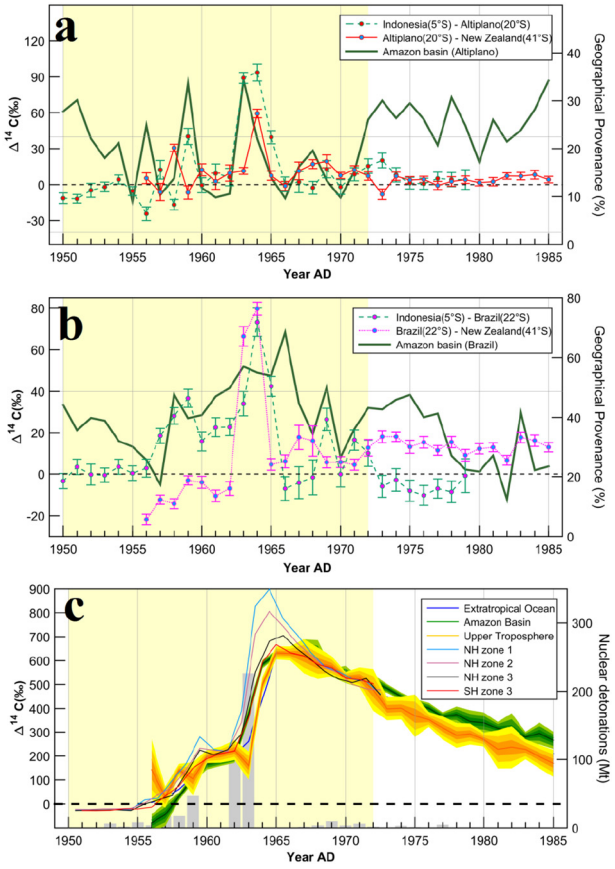

Fig. 5. (a) Comparison between TLPB index I (green dashed line), Extratropical index I (red solid line) and the % of air parcels from the Amazon basin arriving in the Altiplano (green solid line); (b) Comparison between TLPB index II (green dashed line), Extratropical index II (red solid line) and the % of air parcels from the Amazon basin arriving to Southeast Brazil (green solid line); (c) Calculated $\Delta^{14}C$ endmember values for TSA (Extratropical Ocean is the New Zealand atmospheric detrended record) together with radiocarbon latitudinal zones (Hua et al., 2013). Using the errors of each record were calculated the possible maximum and minimum values for the estimation of both Amazon and Upper troposphere endmembers ($\pm$ 1σ, $\pm$ 2σ, and $\pm$ 3σ are represented by shaded colors of the same tinge).The magnitude of nuclear explosions during the bomb-testing period (grey bars, based on Enting, 1982) is also shown. The dashed horizontal line indicates $\Delta^{14}C = 0$. The shaded area highlights the Maximum Gradient Period (MGP).

to isofluxes from these areas on air parcels. Hence, our findings suggest that when comparing the bomb signal in tree-ring records from different latitudes, the disruption on the expected north-south positive $\Delta^{14}C$ gradient global pattern could be associated to the altitude of a record, atmospheric circulation, and the carbon reservoirs upwind to the record.

Data availability

The new Altiplano *P. taparacana* ^{14}C dataset can be found in the supplementary information.

CRediT authorship contribution statement

Santiago Ancapichún: Conceptualization, Methodology, Investigation, Formal analysis, Writing – original draft, Validation, Visualization, Investigation. **Ricardo De Pol-Holz:** Conceptualization, Methodology, Investigation, Writing – original draft, Supervision, Project administration, Funding acquisition. **Duncan A. Christie:** Methodology, Supervision, Investigation, Writing – original draft. **Guaciara M. Santos:** Methodology, Validation, Writing – review & editing. **Silvana Collado-Fabbri:** Methodology, Investigation, Writing – original draft. **René Garreaud:** Methodology, Conceptualization, Writing – review & editing. **Fabrice Lambert:** Writing – review & editing. **Andrea Orfanoz-Cheuquelaf:** Methodology. **Maisa Rojas:** Supervision, Writing – review & editing. **John Southon:** Methodology, Writing – review & editing. **Jocelyn C. Turnbull:** Methodology, Supervision, Writing – review & editing. **Pearce Paul Creasman:** Methodology, Writing – review & editing.

Declaration of competing interest

The authors declare that they have no known competing financial interests or personal relationships that could have appeared to influence the work reported in this paper.

Acknowledgments

We would like to thank all the personnel at the Keck Radiocarbon Facility of the University of California, Irvine for their continuous õsupport and laboratory help. Funding for this study came from the Chilean Agencia Nacional de Investigación y Desarrollo (ANID) Fondecyt grants #1140536, #1201810 and 1201411; ANID FONDAP 15110009 $(CR)^2$ and ICM NC120066. SA was partially supported by the ANID doctoral scholarship 21140194.

References

Anchukaitis, K., Evans, M., Lang, T., Smith, D., Leavitt, S., Schrag, D., 2008. Consequences of a rapid cellulose extraction technique for oxygen isotope and radiocarbon analyses. Anal. Chem. 80 (60), 2035–2041. https://doi.org/10.1021/ac7020272.

Apaéstegui, J., Cruz, F., Vuille, M., Fohlmeister, J., Espinoza, J., Sifeddine, A., et al., 2018. Precipitation changes over the eastern Bolivian Andes inferred from speleothem ($\delta^{18}O$) records for the last 1400 years. Earth and Planetary Letters 494, 124–134. https://doi.org/10.1016/j.epsl.2018.04.048.

Boninsegna, J.A., Argollo, J., Aravena, J.C., Barichivich, J., Christie, D., Ferrero, M.E., et al., 2009. Dendroclimatological reconstructions in South America: a review. Palaeogeography, Palaeoclimatology, Palaeoecology 281 (3-4), 210–228. https://doi.org/10.1016/j.palaeo.2009.07.020.

Braziunas, T., Fung, I., Stuiver, M., 1995. The preindustrial atmospheric $^{14}CO_2$ latitudinal gradients as related to exchanges among atmospheric, oceanic, and terrestrial reservoirs. Glob. Biogeochem. Cycles 9 (4), 565–584. https://doi.org/10.1029/95GB01725.

Broecker, W., Peng, T.-H., Engh, R., 1980. Modeling the carbon system. Radiocarbon 22 (3), 565–598. https://doi.org/10.1017/S0033822200009966.

Capano, M., Miramont, C., Guibal, F., Kromer, B., Tune, T., Fagault, Y., et al., 2017. Wood ^{14}C dating with AixMICADAS: methods and application to tree-ring sequences from the younger Dryas event in the southern French Alps. Radiocarbon 60 (01), 51–74. https://doi.org/10.1017/rdc.2017.83.

Christie, D., Lara, A., Barichivich, J., Villalba, R., Morales, M., Cuq, E., 2009. El Niño-southern oscillation signal in the world's highest-elevation tree-ring chronologies from the Altiplano, Central Andes. Palaeogeogr. Palaeoclimatol. Palaeoecol. 281 (3–4), 309–3019. https://doi.org/10.1016/j.palaeo.2007.11.013.

Draxler, R., Hess, G., 1998. An overview of the HYSPLIT_4 modeling system for trajectories, dispersión, and deposition. Austrian Meteorological Magazine 47, 295–308. https://doi.org/10.1016/S1352-2310(97)00457-3.

Draxler, R., Stunder, J., 1988. Modeling the CAPTEX vertical tracer concentration profiles. J. Appl. Meteorol. 27, 617–625. https://doi.org/10.1175/1520-0450(1988)027<0617:MTCVTC>2.0.CO;2.

Draxler, R., Taylor, D., 1982. Horizontal dispersion parameters for long-range transport modeling. J. Appl. Meteorol. 21, 367–372. https://doi.org/10.1175/1520-0450(1982)021<0367:HDPFLR>2.0.CO;2.

Enting, I., 1982. Nuclear Weapons Data for Use in Carbon Cycle Modeling. Melbourne (Australia), CSIRO Division of atmospheric physics and technology.

Fan, S.-M., Wofsy, S., Bakwin, P., Jacob, D., Fitzjarrald, D., 1990. Atmosphere-biosphere exchange of CO_2 and O_3 in the Central Amazon Forest. J. Geophys. Res.-Atmos. 95, D10. https://doi.org/10.1029/JD095iD10p16851.

Fletcher, R., 1945. The general circulation of the tropical and equatorial atmosphere. J. Meteorol. 2 (3), 167–174. https://doi.org/10.1175/1520-0469(1945)002<0167:TGCOTT>2.0.CO;2.

Garratt, J., 1994. Review: the atmospheric boundary layer. Earth Sci. Rev. 37, 89–134. https://doi.org/10.1016/0012-8252(94)90026-4.

Garreaud, R., 1999. Multiscale analysis of summertime precipitation over the Central Andes. Mon. Weather Rev. 127, 901–921. https://doi.org/10.1175/15200493(1999)127<0901:MAOTSP>2.0.CO;2.

Garreaud, R., Vuille, M., Amy, C., 2003. The climate of the Altiplano: observed current conditions and mechanisms of past changes. Palaeogeogr. Palaeoclimatol. Palaeoecol. 194, 5–22. https://doi.org/10.1016/S0031-0182(03)00269-4.

Garreaud, R., Vuille, M., Compagnucci, R., Marengo, J., 2009. Present-day south American climate. Palaeogeogr. Palaeoclimatol. Palaeoecol. 281, 180–195. https://doi.org/10.1016/j.palaeo.2007.10.032.

Geller, L., Elkins, J., Lobert, J., Clarke, A., Hurst, D., Butler, J., et al., 1997. Tropospheric SF_6: observed latitudinal distribution and trends, derived emissions and interhemispheric exchange time. Geophys. Res. Lett. 24 (6), 675–678. https://doi.org/10.1029/97GL00523.

Graven, H., Guilderson, T., Keeling, R., 2012. Observations of radiocarbon in CO_2 at seven global sampling sites in the Scripps flask network: analysis of spatial gradients and seasonal cycles. J. Geophys. Res. 117, D02303. https://doi.org/10.1029/2011JD016535.

Hastenrath, S., Polzin, D., 2004. Dynamics of the surface wind field over the equatorial Indian Ocean. Q. J. R. Meteorol. Soc. 130, 503–517. https://doi.org/10.1256/qj.03.79.

Heimann, M., Maier-Reimer, E., 1996. On the relations between the oceanic uptake of CO_2 and its carbon isotopes. Glob. Biogeochem. Cycles 10, 89–110. https://doi.org/10.1029/95GB03191.

Held, I., Hou, A., 1980. Nonlinear axially symmetric circulations in a nearly inviscid atmosphere. Journal of the Atmospheric Science 37, 515–533. https://doi.org/10.1175/1520-0469(1980)037<0515:NASCIA>2.0.CO;2.

Hesshaimer, V., Levin, I., 2000. Revision of the stratospheric bomb $^{14}CO_2$ inventory. J. Geophys. Res. 105 (D9), 11641–11658. https://doi.org/10.1029/1999JD901134.

Hou, Y., Zhour, W., Cheng, P., Xiong, X., Du, H., Niu, Z., et al., 2020. ^{14}C-AMS measurements in modern tree rings to trace local fossil fuel-derived CO_2 in the greater Xi'an area, China. Sci. Total Environ. 715, 136669. https://doi.org/10.1016/j.scitotenv.2020.136669.

Hua, Q., Barbetti, M., 2007. Influence of atmospheric circulation on regional $^{14}CO_2$ differences. J. Geophys. Res. 112 (D19). https://doi.org/10.1029/2006jd007898.

Hua, Q., Barbetti, M., Levchenko, V., Arrigo, R., Buckley, B., Smith, A., 2012. Monsoonal influences on southern hemisphere $^{14}CO_2$. Geophys. Res. Lett. 39, L19806. https://doi.org/10.1029/2012GL052971.

Hua, Q., Barbetti, M., Rakowski, A., 2013. Atmospheric radiocarbon for the period 1950-2010. Radiocarbon 55 (4), 2059–2072. https://doi.org/10.2458/azu_js_rc.v55i2.16177.

Hughen, K., Lehman, S., Southon, J., Overpeck, J., Marchal, O., Herring, C., et al., 2004. ^{14}C activity and global carbon cycle changes over the past 50,000 years. Science 303 (5655), 202–207. https://doi.org/10.1126/science.1090300.

Kalnay, E., Kanamitsu, M., Kistler, R., Collins, W., Deaven, D., Gandin, L., et al., 1996. The NCEP/NCAR 40-year reanalysis project. Bull. Am. Meteorol. Soc. 77, 437–471. https://doi.org/10.1175/1520-0477(1996)077<0437:TNYRP>2.0.CO;2.

Key, R., Kozyr, A., Sabine, C., Lee, K., Wanninkhof, R., Bulliste, J., et al., 2004. A global ocean carbon climatology: results from global data analysis project (GLODAP). Glob. Biogeochem. Cycles 18 (4), GB4031. https://doi.org/10.1029/2004gb002247.

Krakauer, N., Randerson, J., Primeau, F., Gruber, N., Menemenlis, D., 2006. Carbon isotope evidence for the latitudinal distribution and wind speed dependence of the air-sea gas transfer velocity. Tellus 58 (B), 390–417. https://doi.org/10.1111/j.1600-0889.2006.00223.x.

Lal, D., Rama, 1966. Charasteristics of global tropospheric mixing based on man-made ^{14}C, ^{3}H, and ^{90}Sr. J. Geophys. Res. 71 (12), 2865–2874. https://doi.org/10.1029/JZ071i012p02865.

Lenters, J., Cook, K., 1997. On the origin of the Bolivian high and related circulation features of south American climate. Journal of the Atmospheric Science 54, 656–677. https://doi.org/10.1175/1520-0469(1997)054<0656:OTOOTB>2.0.CO;2.

Levin, I., Kromer, B., 2004. The tropospheric $^{14}CO_2$ level in mid-latitudes of the northern hemisphere (1959-2003). Radiocarbon 46 (03), 1261–1272. https://doi.org/10.1017/s0033822200033130.

Levin, I., Naegler, T., Kromer, B., Francey, R., Gomez-Pelaez, A., Steele, L., et al., 2010. Observations and modeling of the global distribution and long-term trend of atmospheric $^{14}CO_2$. Tellus 62 (1), 26–46. https://doi.org/10.1111/j.1600-0889.2009.00446.x.

Lima, M., Christie, D.A., Santoro, M.C., Latorre, C., 2016. Coupled socio-environmental changes triggered indigenous Aymara depopulation of the Semiarid Andes of Tarapacá-Chile during the late 19th-20th Centuries. PLOS ONE 11 (8), e0160580. https://doi.org/10.1371/journal.pone.0160580.

Manning, M., Lowe, D., Melhuish, W., Sparks, R., Wallace, G., Brenninkmeijer, C., Mcgil, R., 1990. The use of radiocarbon measurements in atmospheric studies. Radiocarbon 32, 37–58. https://doi.org/10.1017/S0033822200039941.

Messager, C., Speich, S., Key, E., 2012. Marine atmospheric boundary layer over some Southern Ocean fronts during the IPY BGH 2008 cruise. Ocean Sci. 8 (6), 1001–1023. https://doi.org/10.5194/os-8-1001-2012.

Morales, M., Christie, D., Argollo, J., Pacajes, J., Silva, J., Alvarez, C., et al., 2012. Precipitation changes in the south American Altiplano since 1300 AD reconstructed by tree-rings. Clim. Past 8, 653–666. https://doi.org/10.5194/cp-8-653-2012.

Morales, M., Carilla, J., Grau, H.R., Villalba, R., 2015. Multi-century lake area changes in the southern Altiplano: a tree-ring-based reconstruction. Clim. Past 11, 1139–1152. https://doi.org/10.5194/cp-11-1139-2015.

Morales, M.S., Cook, E.R., Barichivich, J., Christie, D.A., Villalba, R., LeQuesne, C., Srur, A.M., Ferrero, M.E., González-Reyes, A., Couvreux, F., Matovsky, V., Aravena, J.C., Lara, A., Mundo, I.A., Rojas, F., Prieto, M.R., Smerdon, J.E., Bianchi, L.O., Masiokas, M.H., Urrutia, R., Rodriguez-Catón, M., Muñoz, A.A., Rojas-Badilla, M., Alvarez, C., Lopez, L., Luckman, B., Lister, D., Harris, I., Jones, P.D., Williams, A.P., Velazquez, G., Aliste, D., Aguilera-Betti, I., Marcotti, E., Flores, F., Muñoz, T., Cuq, E., Boninsegna, J.A., 2020. Six hundred years of south American tree rings reveal an increase in severe hydroclimatic events since mid-20th century. Proc. Natl. Acad. Sci. https://doi.org/10.1073/pnas.2002411117.

Naegler, T., Levin, I., 2009. Observation-based global biospheric excess radiocarbon inventory 1963-2005. J. Geophys. Res. 114, D17302. https://doi.org/10.1029/2008JD011100.

Neukon, R., Rohrer, M., Calanca, P., Salzmann, N., Huggel, C., Acuña, D., et al., 2015. Facing unprecedented drying of the Central Andes? Precipitation variability over the period AD 1000-2100. Environ. Res. Lett. https://doi.org/10.1088/1748-9326/10/8/084017.

Nydal, R., 1968. Further investigation on transfer of radiocarbon in nature. J. Geophys. Res. 73 (12), 3617–3635. https://doi.org/10.1029/JB073i012p03617.

Nydal, R., Lövseth, K., 1965. Distribution of radiocarbon from nuclear tests. Nature 206, 1029–1031. https://doi.org/10.1038/2061029a0.

Oeschger, H., Siegenthaler, U., Schotterer, U., Gugelmann, A., 1975. A box-diffusion model to study the carbon dioxide exchange in nature. Tellus 27 (2), 168–192. https://doi.org/10.1111/j.2153-3490.1975.tb01671.x.

Oliveira, J., Santarosa, E., DePatta, V., Roig, F., 2009. Seasonal cambium activity in the subtropical rain forest tree *Araucaria angustifolia*. Trees 23, 107–115. https://doi.org/10.1007/s00468-008-0259-y.

Oliveira, J., Roig, F., DePatta, V., 2010. Climatic signals in tree-rings of *Araucaria angustifolia* in the southern Brazillian highlands. Austral Ecology 35, 134–147. https://doi.org/10.1111/j.1442-9993.2009.02018.x.

Patra, P., Houweling, S., Krol, M., Bousquet, P., Belikov, D., Bergmann, D., et al., 2011. Transcom model simulations of CH_4 and related species: linking transport, surface flux and chemical loss with CH_4 variability in the troposphere and lower stratosphere. Atmos. Chem. Phys. 11, 12813–12837. https://doi.org/10.5194/acp-11-12813-2011.

Perry, L., Seimon, A., Kelly, G., 2014. Precipitation delivery in the tropical high Andes of southern Peru: new findings and paleoclimatic implications. Int. J. Climatol. 34, 197–215. https://doi.org/10.1002/joc.3679.

Quan, X., Diaz, H., Hoerling, M., 2004. Change in the tropical Hadley cell since 1950. Book: The Hadley Circulation: Present, Past and Future, pp. 85–120 https://doi.org/10.1007/978-1-4020-2944-8_4.

Rafter, T., Fergusson, G., 1959. Atmospheric radiocarbon as a tracer in geophysical circulation problems. United Nations Peaceful Uses of Atomic Energy. Pergamon Press, London.

Randerson, J., Enting, I., Schuur, E., Caldeira, K., Fung, I., 2002. Seasonal and latitudinal variability of troposphere $\Delta^{14}CO_2$: post bomb contributions from fossil fuels, oceans, the stratosphere, and the terrestrial biosphere. Global biochemical Cycles 16 (4), 59–1–59–19. https://doi.org/10.1029/2002GB001876.

Rind, D., Lerner, J., McLinden, C., 2001. Changes of tracer distributions in the doubled CO_2 climate. J. Geophys. Res.-Atmos. 106 (D22), 28061–28079. https://doi.org/10.1029/2001jd000439.

Santos, G., Ormsby, K., 2013. Behavioral variability in ABA chemical pretreatment close to the ^{14}C age limit. Radiocarbon 55 (2), 534–544. https://doi.org/10.1017/S0033822200057660.

Santos, G., Southon, J., Druffel-Rodriguez, K., Griffin, M., Mazon, M., 2004. Magnesium perchlorate as an alternative water trap in AMS graphite simple preparation: a report on sample preparation at KCCAMS at the University of California, Irvine. Radiocarbon 46 (1), 165–173. https://doi.org/10.1017/S0033822200039485.

Santos, G., Moore, R., Southon, J., Griffin, S., Hinger, E., Zhang, D., 2007. AMS ^{14}C sample preparation at the KCCAMS/UCI facility: status report and performance of small samples. Radiocarbon 49 (2), 255–270. https://doi.org/10.1017/S0033822200042181.

Santos, G., Linares, R., Lisi, C., Tomazello, M., 2015. Annual growth rings in a simple of Pananá pine (*Araucaria angustifolia*): toward improving the ^{14}C calibration curve for the southern hemisphere. Quat. Geochronol. 25, 96–103. https://doi.org/10.1016/j.quageo.2014.10.004.

Santos, G., Granato-Souza, D., Maioli, A., Oelkers, R., Andreu-Hayles, L., 2020. Radiocarbon analysis confirms anual periodicity in *Cedrela odorata* tree rings from the equatorial Amazon. Quat. Geochronol. 28, 101079. https://doi.org/10.1016/j.quageo.2020.101079.

Scarchilli, C., Frezzotti, M., Ruti, P., 2011. Snow precipitation at four ice core sites in East Antarctica: provenance seasonality a blocking factors. Clim. Dyn. 37, 2107–2125. https://doi.org/10.1007/s00382-010-0946-4.

Schlosser, E., Oeter, H., Mason-Delmonte, V., Reijmer, C., 2008. Atmospheric influence on the deuterium excess signal in polar firn: implications for ice-core interpretation. J. Glaciol. 54, 117–124. https://doi.org/10.3189/002214308784408991.

Segura, H., Espinoza, J., Junquas, C., Lebel, T., Vuille, M., Garreaud, R., 2020. Recent changes in the precipitation-driving processes over the southern tropical Andes/western Amazon. Clim. Dyn. https://doi.org/10.1007/s00382-020-05132-6.

Solíz, C., Villalba, R., Argollo, J., Morales, M.S., Christie, D.A., Moya, J., Pacajes, J., 2009. Spatio-temporal variations in Polylepis tarapacana radial growth across the Bolivian Altiplano during the 20th century. Palaeogeography, Palaeoclimatology, Palaeoecology 281 (3-4), 296–308. https://doi.org/10.1016/j.palaeo.2008.07.025.

Southon, J., Magana, A., 2010. A comparison of cellulose extraction and ABA pretreatment methods for AMS ^{14}C dating of ancient wood. Radiocarbon 52 (3), 1371–1379. https://doi.org/10.1017/S0033822200046452.

Stein, A., Draxler, R., Rolph, G., Stunder, B., Cohen, M., Ngan, F., 2015. NOAA's HYSPLIT atmospheric transport and dispersion modeling system. Bull. Am. Meteorol. Soc. 96, 2059–2077. https://doi.org/10.1175/BAMS-D-14-00110.1.

Stuiver, M., Polach, H., 1977. Discussion: reporting of ^{14}C data. Radiocarbon 19 (3), 355–363. https://doi.org/10.1017/S0033822200003672.

Tomas, R., Holton, J., Webster, P., 1999. The influence of cross-equatorial pressure gradients on the location of near-equatorial convection. Q. J. R. Meteorol. Soc. 125, 1107–1127. https://doi.org/10.1002/qj.1999.49712555603.

Turnbull, J., Miller, J., Lehman, S., Tans, P., Sparks, R., Southon, J., 2006. Comparison of $^{14}CO_2$, CO and SF_6 as tracers for determination of recently added fossil fuel CO_2 in the atmosphere and implications for biological CO_2 exchange. Geophys. Res. Lett. 33, L01817. https://doi.org/10.1029/2005GL024213.

Turnbull, J., Rayner, P., Miller, J., Naegler, T., Ciais, P., Cozic, A., 2009. On the use of $^{14}CO_2$ as a tracer for fossil fuel CO_2: quantifying uncertainties using an atmospheric transport model. J. Geophys. Res. 114, D22302. https://doi.org/10.1029/2009JD012308.

Turnbull, J., Mikaloff, S., Ansell, I., Brailsford, G., Moss, R., Norris, M., et al., 2017. Sixty years of radiocarbon dioxide measurements at Wellington, New Zealand: 1954-2014. Atmos. Chem. Phys. 17, 14771–14784. https://doi.org/10.5194/acp-17-14771-2017.

Turnbull, J.C., Graven, H.D., Krakauer, N.Y., 2016. Radiocarbon in the atmosphere. In: Schuur, E.A.G., Druffel, E.R.M., Trumbore, S.E. (Eds.), Radiocarbon and Climate Change. Springer International Publishing, pp. 83–137.

Vera, C., Diaz, L., Saurral, R., 2019. Influence of anthropogenically-forced global warming and natural climate variability in the rainfall changes observed over the south American Altiplano. Frontiers in Environmental Science https://doi.org/10.3389/fenvs.2019.00087.

Vuille, M., Keimig, F., 2004. Interannual variability of summertime convective cloudiness and precipitation in the central Andes derived from ISCCP-B3 data. J. Clim. 17, 3334–3348. https://doi.org/10.1175/1520-0442(2004)017<3334:IVOSCC>2.0.CO;2.

Vuille, M., Bradley, R., Keimig, F., 2000. Interannual climate variability in the Central Andes and its relation to tropical Pacific and Atlantic forcing. J. Geophys. Res. 105, 12447–12460. https://doi.org/10.1029/2000JD900134.

Vuille, M., Burns, S., Taylor, B., Cruz, F., Bird, B., Abbott, M., et al., 2012. A review of the South American monsoon history as recorded in stable isotopic proxies over the past two millennia. Clim. Past 8, 1309–1321. https://doi.org/10.5194/cp-8-1309-2012.

Zeng, X., Brunke, M., Zhou, M., Fairall, C., Bond, N., Lenschow, D., et al., 2004. Marine atmospheric boundary layer height over the eastern Pacific: data analysis and model evaluation. J. Clim. 17, 4159–4170. https://doi.org/10.1175/JCLI3190.1.